MODELING WOUND ROLLS USING EXPLICIT FE METHODS

by

B. K. Kandadai and J. K. Good
Oklahoma State University
USA

ABSTRACT

A new method of wound roll analysis using an explicit finite element formulation is presented in this paper. The stresses developed in center wound rolls with and without an undriven nip roller are discussed and compared with analyses found in literature. For center wound rolls with an undriven nip roller, the results show that the Nip-Induced-Tension (NIT) is proportional to the coefficient of friction between web layers and the nip load. The NIT is also found to be independent of the web tension. The conditions of slip that exist between the layers in the wound roll, the effect of start-up web to core discontinuities, advantages and limitations of this modeling technique have also been discussed.

NOMENCLATURE

$A(t)$	Amplitude ratio as a function of time 't'
A_s, A_f	Starting, Final amplitude values respectively
b_1, b_2	Linear, Quadratic bulk viscosity coefficients respectively
C_d, E	Dilatational wave speed, Young's modulus
L^e, $L_{\min}$	Elemental length, Minimum elemental length
N, NIT	Nip load, Nip-Induced-Tension
$p(x)$	Pressure acting on the surface of a given layer
P_l, P_q	Linear, Quadratic bulk viscosity respectively
$q_t(x)$, $q_b(x)$	Top and Bottom surface tractions acting on a given layer
r, u	Radius, Distance from the neutral axis of the web
t_s, t_f	Starting, Final time values respectively
T_w	Web tension
WOT	Wound-on-Tension
Δt	Stable time increment
$\dot{\varepsilon}_{vol}$, ε_r, ε_θ	Volumetric, Radial and Tangential strain respectively
λ, μ	Lame's constants (context)
μ_{WW}	Kinetic coefficient of friction between web layers

μ_{WN}	Kinetic coefficient of friction between the web and nip roller
μ_{WC}	Kinetic coefficient of friction between the web and core
ν	Poisson's ratio
$\xi(t)$	Ratio of time difference as a function of time 't'
ρ, σ	Mass density, stress
τ, τ_{crit}	Shear stress, Critical shear stress
σ_r, σ_θ	Radial, Tangential stresses respectively
ω_c, $\omega_{\max}$	Core angular velocity, Maximum frequency of the stress wave

INTRODUCTION

Analysis of the wound roll structure has been carried out since the 1950s. Theoretical investigations on the wound roll structure and the wound roll models can broadly be classified into the following categories based on the solution approach:

- Closed form solutions based on linear elastic small deformation theory
- Approximate solutions based on energy methods
- Numerical solutions based on linear elastic small deformation theory, viscoelastic and thermoelastic formulations and large deformation continuum approach
- Numerical solutions based on accretive axi-symmetric finite element formulations
- Numerical solutions with the use of commercial finite element (FE) codes

Many of the analytical and numerical models classified above have been reviewed by Good [1] and by Roisum [2]. Only a few authors have focused on analysis of wound rolls using FE methods. Hoffecker and Good [3] used a static axisymmetric finite element accretive formulation to determine the stress distribution inside a wound roll. This model allows for widthwise variations in web thickness and uses multi-point constraints to compute the stresses in each lap due to addition of the incoming layer. The addition of a new layer is analogous to the classic press fit problem where a contact pressure between two cylinders is developed due to radial interference. Lee and Wickert [4] used a similar approach to predict the wound roll stresses. The difference between Hoffecker's and Lee's model lies in the allocation of the web tension in the incoming web layer. In Hoffecker's model, the web tension is allocated based upon the widthwise variation in radius of the previous lap that was added to the roll. Lee's model does not allow any variation in radius across the width to impact the allocation of tension.

Commercial FE codes have primarily been used to study the effect of roll weight, gravity, etc on the wound roll structure. Some of the examples include the coil collapse FE simulations of Smolinski et al [5] and Li and Cao [6]. Arola and von Hertzen [7] analyzed the development of sheet tension under a rolling nip on a paper stack using explicit FE methods. Recently, in another study [8], Arola and von Hertzen used an elastoplastic continuum model in an explicit formulation to study the slippage within the wound roll. The same model was extended to study the effect of clamping forces on the deformation of the wound rolls. Be it a classical or a numerical approach, all the authors have assumed that the wound roll is a set of concentric hoops. In reality the wound roll resembles an Archimedean spiral. In order to analyze the problem that includes the spiral nature of the wound roll and allow for the discontinuity near the core, an explicit formulation is necessary.

WOUND ROLL FE MODEL

In a typical winding process, during the start of winding, the incoming pre-tensioned layer is fastened to the core and layers are wound on top of the core. Depending on the type of the winding process, winding is accomplished by providing torque to the core shaft (center winding) or to the drum (surface winding).

Model Set Up

The model is set up such that it resembles a real winding process closely. Consider an initial configuration in which the incoming web layer is tied to the rigid core as shown in Figure 1a. The core and the nip roller (in the case of center winding with an undriven nip roller) are modeled as rigid cylindrical bodies. The web is modeled as an elastic layer of constant thickness. Winding is then accomplished in different steps that are a function of time in ABAQUS/Explicit® (a commercial FE program).

In the first time step, a known value of load (distributed load 'T_w' at the end of the sheet) is prescribed at the left end of the sheet. This simulates the web tension in the incoming sheet as shown in Figure 1b. In this time step, the center of rotation of the core is fixed in all degrees of freedom while the nip roller is pinned. In the second time step, the nip roller contacts the incoming web under a prescribed nip load 'N'. In this time step, the boundary conditions are modified such that the center of rotation of the nip roller is fixed only in the horizontal degree of freedom and is free to move vertically as well as rotate about its axis as shown in Figure 1c. This facilitates the application of nip load vertically. In the case of center winding without an undriven nip roller, this step is not present. In the third step (second for center winding without an undriven nip roller), winding of the roll is accomplished by prescribing an angular velocity to the rigid core as shown in Figure 1d. Also, the rotational constraint on the rigid core is removed during this step to facilitate the winding process. The model properties are summarized in Table 1.

Property	Value
Web length	509.5 cm (200 in)
Web thickness (Caliper)	0.254 cm (0.1 in)
Rigid core diameter	8.89 cm (3.5 in)
Rigid nip roller diameter	10.16 cm (4 in)
Angular velocity (ω_c)	0.5 rad/sec
Coefficient of friction ($\mu_{N/w}$, $\mu_{w/w}$, $\mu_{c/w}$)	0.2, 0.2, 0.2
Web tension (T_w)	2.6, 4.4, 6.1 N/cm
Nip load (N)	8.8, 17.5, 26.3, 35 N/cm
Young's modulus (E), Poisson's ratio (v)	69 MPa (10,000 Psi), 0.3

Table 1: Winding model properties.

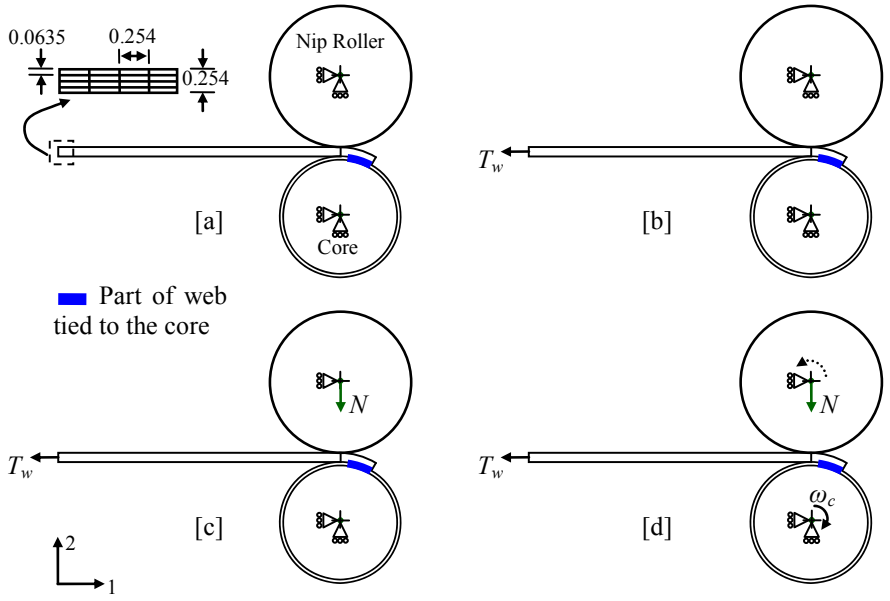

Figure 1 – Schematic representation of the FE model set up

Element and Material Constitutive Behavior

The winding problem is analyzed in plane stress conditions. The core and the nip roller are modeled as rigid analytical surfaces. In order to model the elastic web, ABAQUS/Explicit® has four-noded isoparametric quadrilateral elements for two-dimensional explicit dynamic analysis in both full and reduced integration types. However the reduced integration elements offer significant computational advantages as the strains and stresses are computed only at one integration point instead of four [9]. Superficially this appears to be a poor approximation, but it has proved to offer significant advantages. For first-order elements the uniform strain method yields the exact average strain over the element volume. Not only is this important with respect to the values available for output, it is also significant when the constitutive model is nonlinear, since the strains passed into the constitutive routines are a better representation of the actual strains. However, this also means that, if a single element is used to model the thickness of a layer, the strains and stresses through the depth of the layer would be uniform. If bending of the layer is to be simulated it is necessary to use at least two elements through the depth of the web. The stresses and strains obtained at integration points (same as the centroid for reduced integration elements) will have to be extrapolated in order to compute the surface strains and stresses. A uniform meshing scheme is used to model the web. The winding model consists of 8,026 nodes and 10,036 elements with 20,073 degrees of freedom.

It is well known that webs wound into rolls behave as anisotropic bodies. Also, the radial modulus property which is measured as the modulus of a web stack is a nonlinear quantity and varies with pressure. However, in order to keep the problem simple and the computational time less, the web is modeled as a linear isotropic material and the stresses and strains are assumed to follow the constitutive relationship in plane stress as

expressed in Equation {1}. The modulus of elasticity and Poisson's ratio of the web material are chosen to be 69 MPa and 0.3 respectively.

$$\begin{Bmatrix} \varepsilon_r \\ \varepsilon_\theta \\ \gamma_{r\theta} \end{Bmatrix} = \frac{1}{E} \begin{bmatrix} 1 & -\nu & 0 \\ -\nu & 1 & 0 \\ 0 & 0 & 2(1+\nu) \end{bmatrix} \begin{Bmatrix} \sigma_r \\ \sigma_\theta \\ \tau_{r\theta} \end{Bmatrix} \quad \{1\}$$

Surface Interactions and Contact Modeling

At the start of the winding process, the bottom surface of the incoming web layer contacts the rigid core. After one revolution of the core, the bottom surface of the incoming web layer contacts the top surface of the winding roll. In case of winding with an undriven nip roller, the top surface of the incoming web layer contacts the rigid nip surface. Thus, one of the challenges in modeling a winding process using an explicit FE method is to accurately model the surface interactions. This is accomplished by modeling the contact pairs using a kinematic predictor-corrector contact algorithm [10] to strictly enforce the contact constraints that allows for no nodal penetrations. The kinematic contact algorithm is used for modeling the surface interaction between the nip roller and the wound roll and also between the web layers. A penalty contact algorithm is used to define the contact between the web surface and the rigid core. This is necessary as multi-point constraints are employed between the web surface and the rigid core to simulate the adhesive used to tack the web to the core.

The interaction between contacting surfaces consists of two components: one normal to the surfaces and one tangential to the surfaces. The tangential component consists of the relative motion between the surfaces and the frictional shear stresses. The normal component consists of the penetration between the surfaces. The normal contact is handled using a hard contact model which assumes that the surfaces transmit no contact pressure unless the surfaces involved are in contact. When in contact, there is no limit on the contact pressure that can be transmitted between the surfaces. The surfaces separate if the contact pressure reduces to zero and separated surfaces can come back into contact when the clearance between them reduces to zero. When surfaces are in contact they can transmit shear as well as normal forces across their interface. The relationship between the two force components is expressed in terms of the stresses at the interface of the bodies. The tangential behavior between all contacting surfaces is modeled using a balanced kinematic master-slave contact algorithm with finite sliding. The finite sliding formulation allows for any arbitrary motion between the surfaces involved. The friction between all contacting surfaces is modeled using the Coulomb's friction law with a constant coefficient of friction. The Coulomb friction model relates the maximum allowable frictional (shear) stress across an interface to the contact pressure between the contacting bodies. In the basic form of the Coulomb friction model, two contacting surfaces can carry shear stresses up to a certain magnitude across their interface prior to sliding relative to one another; this state is known as sticking. This is schematically represented in Figure 2.

The Coulomb friction model defines this critical shear stress 'τ_{crit}' as the stress at which sliding of the surfaces starts as a fraction of the contact pressure '*p(x)*' between the surfaces as given in Equation {2}. The stick/slip calculations determine when a point in a contact region moves from sticking to slipping or from slipping to sticking.

$$\tau_{crit} = \mu\, p(x) \quad \{2\}$$

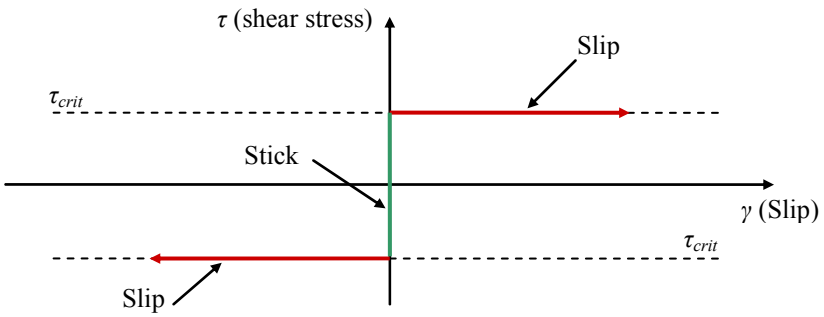

Figure 2 – Schematic representation of a Coulomb friction model.

Loading Rates and Damping

For accuracy and efficiency, quasi-static analysis requires the application of loading that is as smooth as possible. Sudden, jerky movements cause stress waves, which can induce noisy or inaccurate solutions. Applying the load in the smoothest possible manner requires that the acceleration changes only a small amount from one increment to the next. If the acceleration is smooth, it follows that the changes in velocity and displacement are also smooth. In order to reduce the oscillatory behavior of these parameters, the velocity and load boundary conditions are ramped to their final values smoothly and are calculated using Equation {3} [11]. The boundary conditions in the model are shown as a function of time in Figure 3.

$$A(t) = A_s + (A_f - A_s)\xi(t)^3\left(10 - 15\xi(t) + 6\xi(t)^2\right) \;;\; \xi(t) = \frac{t - t_s}{t_f - t_s} \qquad \{3\}$$

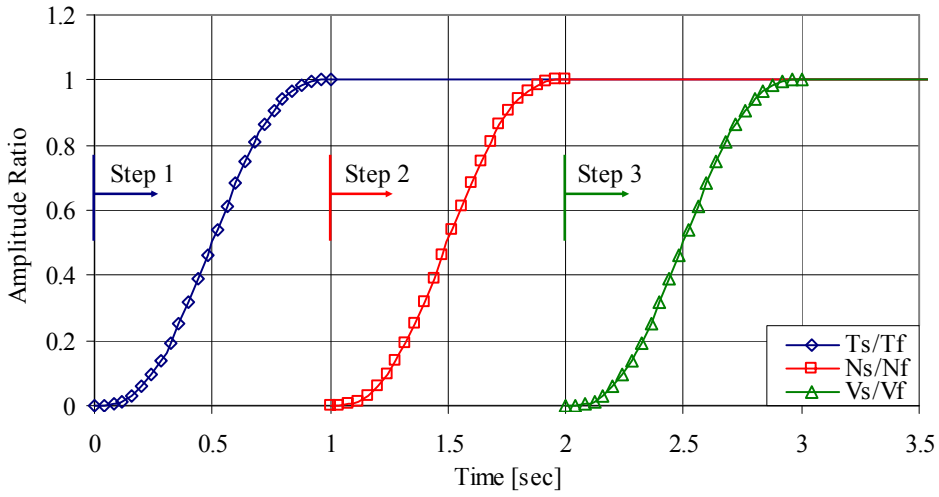

Figure 3 – Behavior of web tension, nip load and core surface velocities as a function of individual step times.

Typically, damping is used for two reasons in dynamics analysis. One is to limit the numerical oscillations in the system and the other is when physical damping is required. ABAQUS/Explicit adds a bulk viscosity damping to the model by default. The bulk viscosity introduces damping associated with the volumetric straining. Its purpose is to improve the modeling of high-speed dynamic events. The bulk viscosity pressure is not included in the material point stresses because it is intended as a numerical effect only. It is not considered to be a part of the material's constitutive response. There are two forms of bulk viscosity in ABAQUS/Explicit. The first is found in all elements and is introduced to damp the "ringing" in the highest element frequency. This damping is sometimes referred to as truncation frequency damping. It generates a bulk viscosity pressure, which is linear in the volumetric strain and is given in Equation {4}. The second form of bulk viscosity pressure is quadratic in the volumetric strain rate and is applied only if the volumetric strain rate is compressive and is given in Equation {5}. The default values for 'b_1' and 'b_2' in ABAQUS/Explicit® are 0.06 and 1.2 respectively and are used for analysis. Since the time period of loading is very long compared to the periods of the natural frequencies of the model, the damping factors do not affect the solution appreciably. Increasing or decreasing the damping factors by a factor of 10 does not change the solution appreciably and the maximum error was less than 1%.

$$p_1 = b_1 \rho c_d L^e \dot{\varepsilon}_{vol} \qquad \{4\}$$

$$p_q = \rho\left(b_2 L^e\right)^2 \left|\dot{\varepsilon}_{vol}\right| min\left(0, \dot{\varepsilon}_{vol}\right) \qquad \{5\}$$

Solution Accuracy and Computational Aspects

The explicit procedure integrates through time by using many small time increments. The time increment is based on the central difference operator that is only conditionally stable. The stability limit is the largest time increment that can be used without generating large, rapidly growing errors. It is closely related to the time required for a stress wave to cross the smallest element dimension in the model and is expressed in terms of the highest frequency of the system as given in Equation {6}. An approximation to the stability limit is written as the smallest transit time of a dilatational wave across any of the elements in the mesh as given in Equation {7}. Thus, the time increment in an explicit dynamic analysis can be very short if the mesh contains small elements or if the stress wave speed in the material is very high.

$$\Delta t \geq \frac{2}{\omega_{\max}} \qquad \{6\}$$

$$\Delta t \approx \frac{L_{\min}}{C_d};\ C_d = \sqrt{\frac{\lambda + 2\mu}{\rho}};\ \lambda = \frac{E\nu}{(1+\nu)(1-2\nu)};\ \mu = \frac{E}{2(1+\nu)} \qquad \{7\}$$

Because the explicit central difference method is used to integrate the equations in time, the discrete mass matrix used in the equilibrium equations plays a crucial role in both computational efficiency and accuracy for both classes of problems [12]. Mass scaling is the procedure of increasing the mass of the entire or partial structure such that the smallest stable time increment can be increased to reduce the overall computational

time. As can be inferred from Equation {7}, the stable time increment is directly proportional to the square root of density. When a mass scaling factor of 'f' is used, the stable time increment increases by √f. When used appropriately, mass scaling can often improve the computational efficiency while retaining the necessary degree of accuracy required for a particular problem [13]. It should be ensured that the changes in the mass and consequent increases in the inertial forces do not alter the solution significantly. Since the stable time increment is also dependent on the smallest elemental dimension, choice of the elemental dimensions and mesh schemes can play an important role in both the accuracy and computational time.

In the winding FE model, the element length, width and mass scaling factors are carefully chosen and set at 0.254 cm, 0.0635 cm and 50 respectively. A typical wound roll is made up of many layers (often thousands). However winding an entire roll in ABAQUS/Explicit® is computationally expensive. In order to study the winding problem and get a basic understanding of the development of wound roll stresses the wound roll finite element model is run till 13 layers are wound onto a rigid core. The analysis takes on an average of 60 hours to complete. Desktop computers with average processing capabilities equivalent to that of an Intel Pentium IV® 3.0 GHz processor with 1 Megabyte of RAM were used for model simulations.

FE MODEL RESULTS: WOUND ROLL STRESSES

At the end of the winding process, in the last time step, the radial pressure in the wound roll as a function of wound roll length is shown in Figure 4. The radial pressure shown in the figure is calculated as the average of the centroidal stresses through the depth of each layer in the wound roll. The radial pressure in a given lap is oscillatory and the magnitude of these oscillations reduces in the laps away from the core. The tangential stress in any layer within the wound roll is comprised of both the membrane stress and the bending stress. The top and the bottom surface tangential stresses in the wound roll as a function of wound roll length are shown in Figure 5. Observe that the bending stress in the layer is significant and can be calculated using the strain-displacement relation [14] given in Equation {8}.

The membrane portion of the tangential stress in a given layer can be calculated as the average of the top and bottom surface stresses and is shown in Figure 6. The tangential stress behavior is noisier near the core and the magnitude of the oscillations decreases with increase in wound roll length. At the outer diameter, the tangential stress is equivalent to the web tension in the free span. In the case of center winding with a nip roller, the qualitative behavior of both the radial and the tangential stresses remains the same; however the quantitative values differ. Similarly, the qualitative behavior of the stresses remains the same at different values of web tension and nip load but the quantitative values differ.

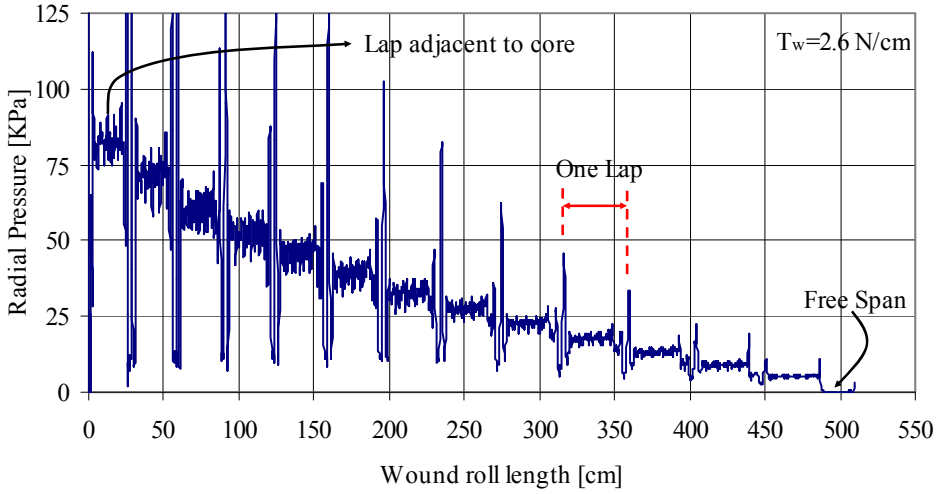

Figure 4 – Radial pressure inside the wound roll

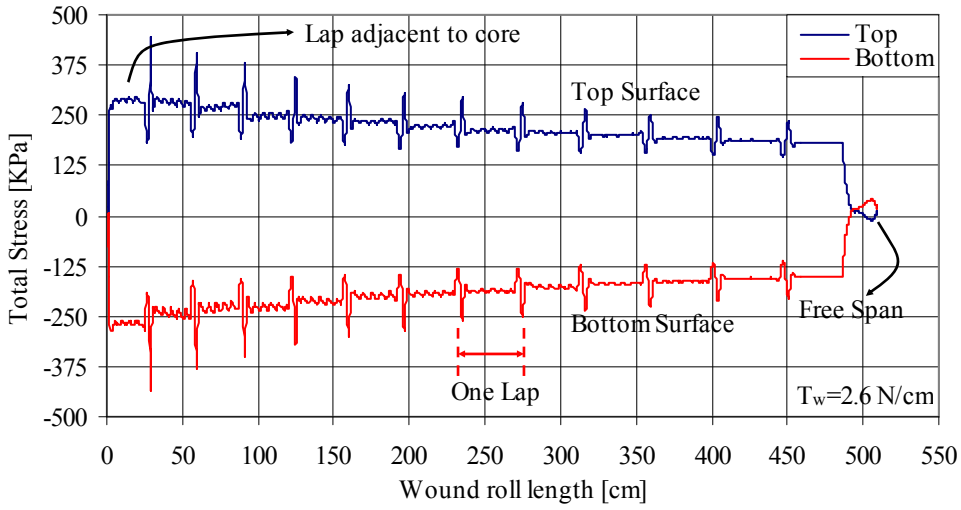

Figure 5 – Total stresses in the top and bottom surface of each layer in the wound roll

$$\sigma_{Bending\ Stress} = E.\frac{u}{r} \qquad \{8\}$$

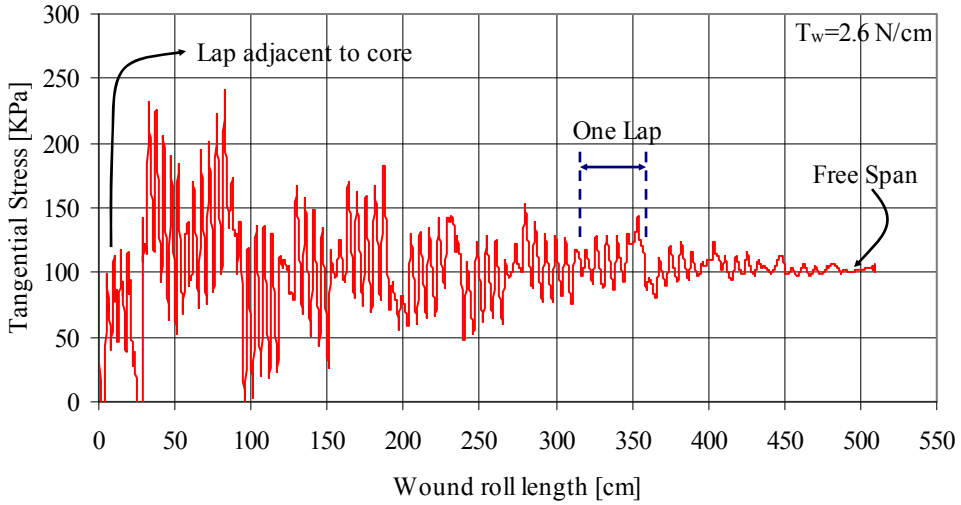

Figure 6 – Tangential stresses in each lap in the wound roll

FE MODEL RESULTS: VERIFICATION

The model results for radial pressure and tangential stresses are compared to the results obtained using Hakiel's model [15] in and Figure 8 respectively. Observe that the FE model results represent the average of the radial pressure and the tangential stress values in each lap. The radial pressure and tangential stress values from the FE model compare well to the Hakiel's model results except near the core.

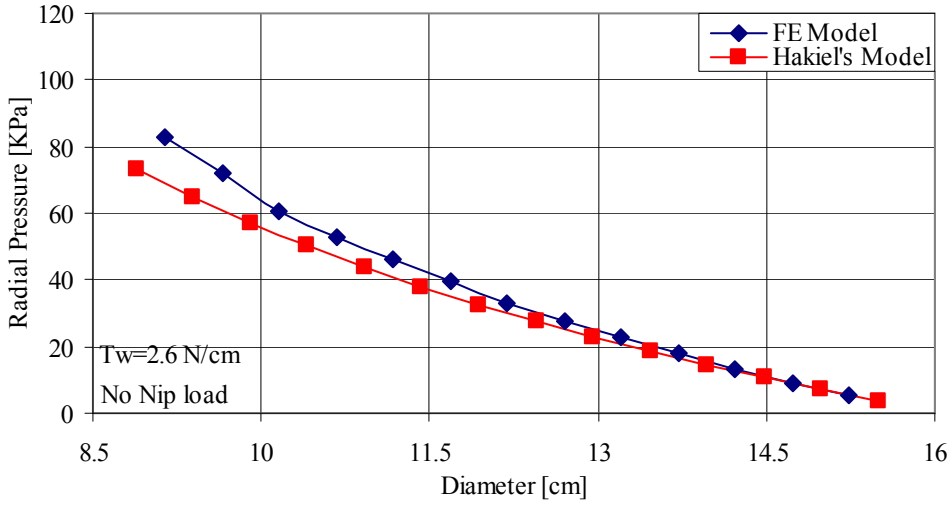

Figure 7 – Comparison of radial pressure between the FE model and Hakiel's model.

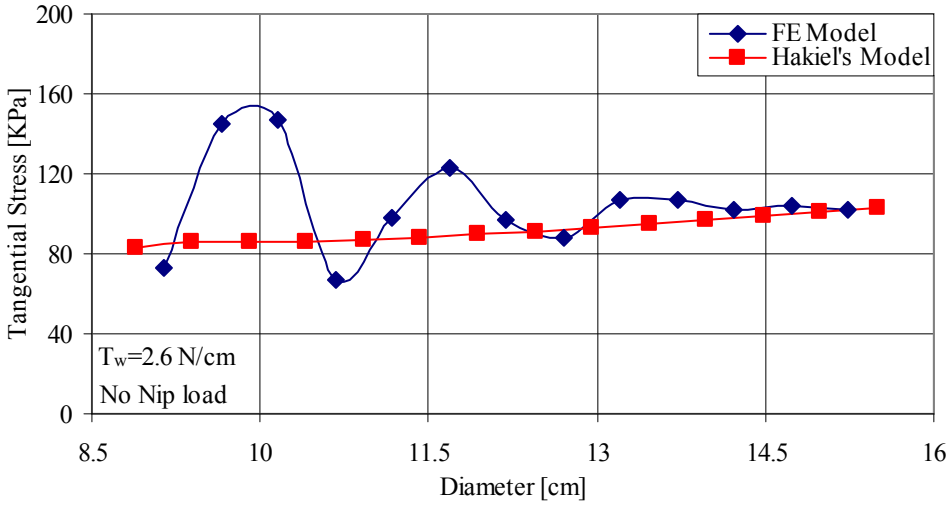

Figure 8 – Comparison of tangential stresses between the FE model and the Hakiel's model.

As a new lap is laid on top of the layer adjacent to the core, the new lap encounters a radial discontinuity at the end of the part of the web layer that is tied to the core as shown in Figure 9. This creates a severe stress concentration and thus the average stresses in the laps are higher than that is calculated using Hakiel's model. Note that Hakiel's model incorporates an assumption that each lap in a wound roll is modeled as a concentric hoop and no discontinuities occur within the wound roll. Also Hakiel's model is a one dimensional solution that provides the radial and tangential stresses as a function only of wound roll radius. As such discontinuities in a circumferential direction cannot be explored with Hakiel's model but in fact these discontinuities do exist. The stress concentration causes the spikes in radial pressure and tangential stress values discussed in section 3. As the roll grows, the stress concentration decreases, the wound roll becomes more cylindrical and hence, the radial pressure values compare well between the FE model and Hakiel's model.

The equilibrium equation for a hoop under plane stress condition in cylindrical coordinates [16] is given in Equation {9}. The tangential stress in each layer calculated from the average radial pressure in the wound roll is compared with the tangential stress values shown in Figure 10. Observe that a very small change in the slope due to the changes in radial pressure values near the core can cause significant changes in the tangential stresses.

$$r\frac{d\sigma_r}{dr}+\sigma_r-\sigma_t=0 \qquad \{9\}$$

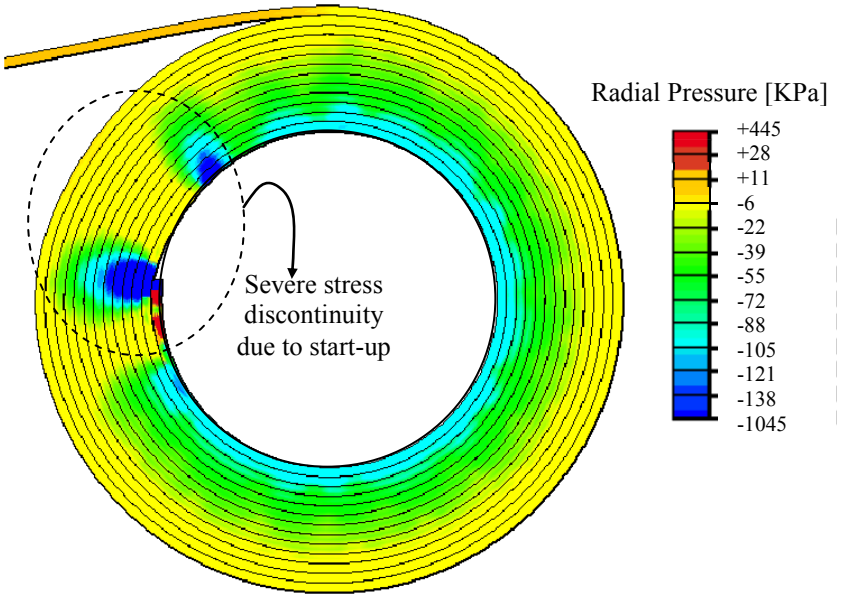

Figure 9 – Stress discontinuity near the core due to web thickness

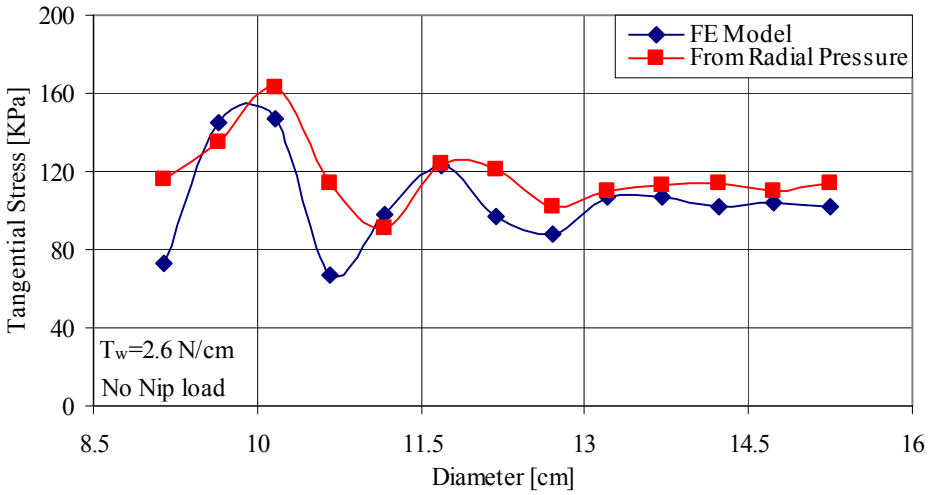

Figure 10 – Comparison of tangential stress output from the FE model and from Equation {9}.

EFFECT OF NIP LOAD AND WEB TENSION

The effect of nip load on wound roll pressures and tangential stresses in a center wound roll with an undriven nip roller at a constant web tension of 2.63 N/cm is shown in Figure 11. Although the results are not shown here, increasing the web tension

increases the wound roll stresses and results in a similar qualitative behavior as shown in Figure 11. Similar observations have been made by Good and Fikes [17]. The web tension and the nip load control the tangential stresses in the outermost layer which in turn controls the stresses inside the wound roll. The tension in the outermost layer of a winding roll is commonly referred to as the wound-on-tension (WOT).

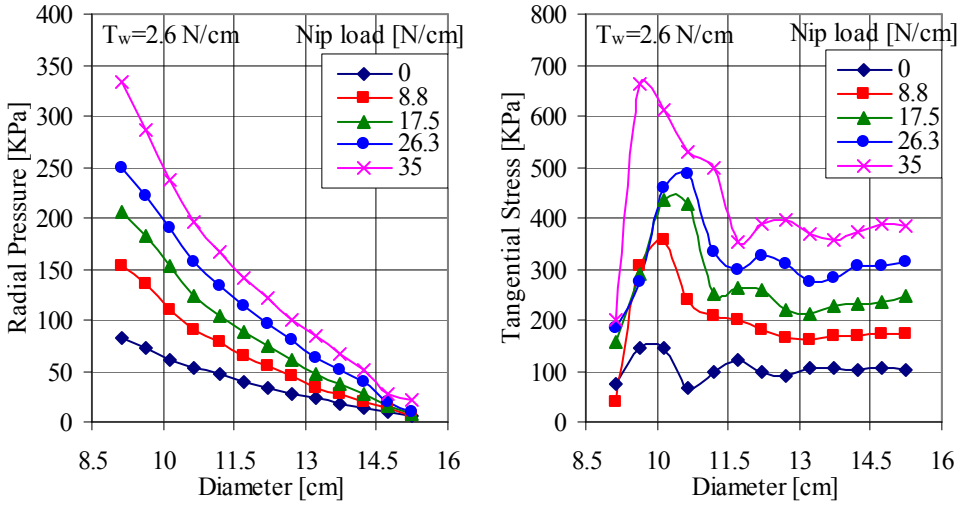

Figure 11 – Effect of nip load on wound roll stresses

The WOT is expressed in terms of force per unit width of web with units of N/cm and is calculated by multiplying the average tangential stress in the outermost layer and the thickness of the layer. The effect of web tension and nip load on the WOT is shown in Figure 12. In this case, observe that the WOT varies linearly with both the web tension and the nip load. As the web tension increases, the WOT values at different nip loads are linearly displaced by the amount of increase in web tension. The nip-induced-tension (NIT) is the component of the WOT that is caused due to the nip load and can be calculated by subtracting the value of web tension from the WOT when center winding with an undriven nip roller. The figure indicates that the NIT is independent of web tension in a center winding process with an undriven nip roller. When the slope of the NIT curve is calculated a value of 0.2 is obtained and this value is equivalent to the kinetic coefficient of friction between the web layers that is given as an input to the model. This is similar to the observations of Good et al [18]. They also observed that the WOT reduces from the maximum possible value of 'μN' at high values of nip load.

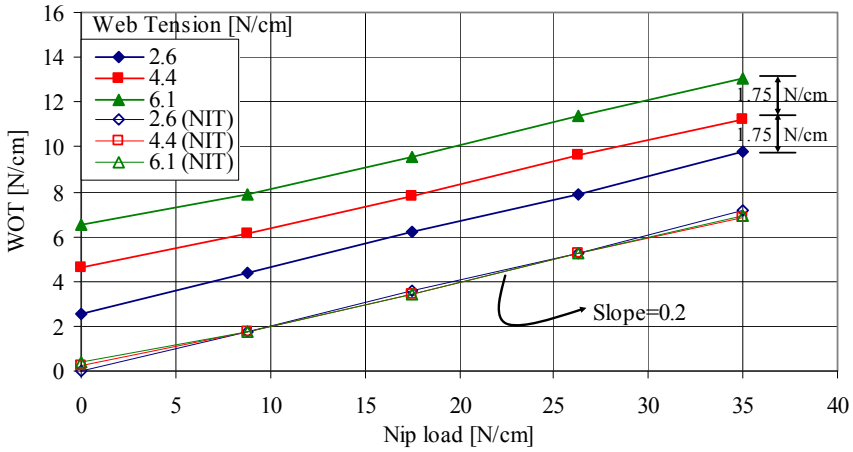

Figure 12 – Effect of web tension and nip load on the WOT and NIT

BEHAVIOR OF SURFACE TRACTIONS

In order to understand the nature of the behavior of surface tractions, it is important to understand the forces acting on a layer inside a wound roll. Consider the top surface of a layer within the wound roll as shown in Figure 13a. Due to the presence of layers on top and bottom, a pressure acts perpendicular to the top and bottom surface of the layer under consideration. Due to the contact mechanics between the layers, traction forces exist on the surfaces of the layer. Since the contact between the layers is modeled using the Coulomb model, the maximum traction a layer can sustain is equivalent to $\pm \mu p(x)$. When the traction forces on a given surface reach the maximum value (i.e. when they fall on the envelopes of $\pm \mu p(x)$) as shown in Figure 13b, the surface is under a condition of slip and when the traction values are less than $\pm \mu p(x)$ (i.e. when they fall between the envelopes of $\pm \mu p(x)$), the surface is under a condition of stick. When under stick, the relative motion and hence, the relative velocity between the surfaces in contact becomes zero.

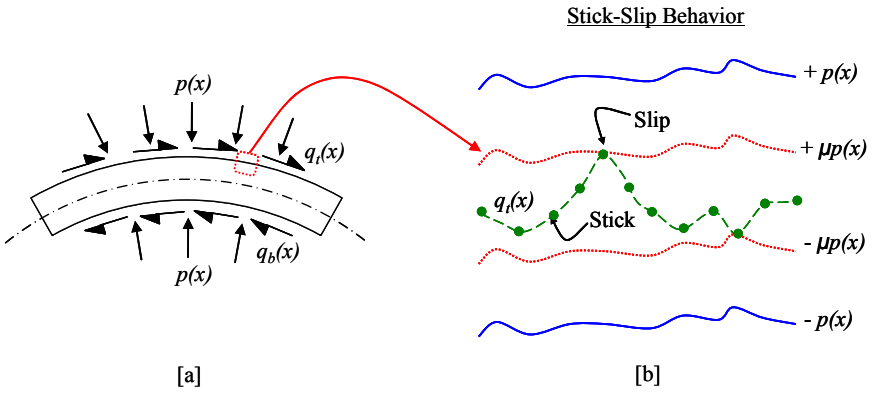

Figure 13 – Behavior of surface tractions in a given layer inside the wound roll

The behavior of the bottom and the top surface tractions of the web inside the wound roll is shown in Figure 14 and Figure 15. Observe that surface tractions are shown for only five layers adjacent to the core. The contact pressure between the layers decreases away from the core and hence the envelope progressively reduces to the outer diameter of the wound roll. The surface tractions in the bottom surface of the web layer adjacent to the core is under stick and is noisy due to the use of penalty contact algorithm between the web surface and the rigid core surface. This noise is not observed in the top surface traction as it the layer-layer contact is modeled using a kinematic contact algorithm. Also, elsewhere in the roll, a repeatable pattern in slip-stick behavior is observed in both the top and bottom surfaces.

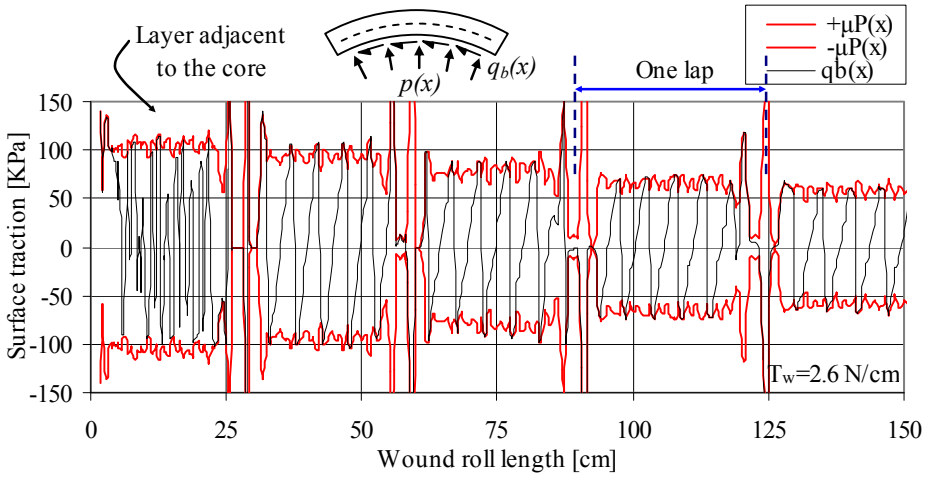

Figure 14 – Behavior of the bottom surface tractions in the layers near the core

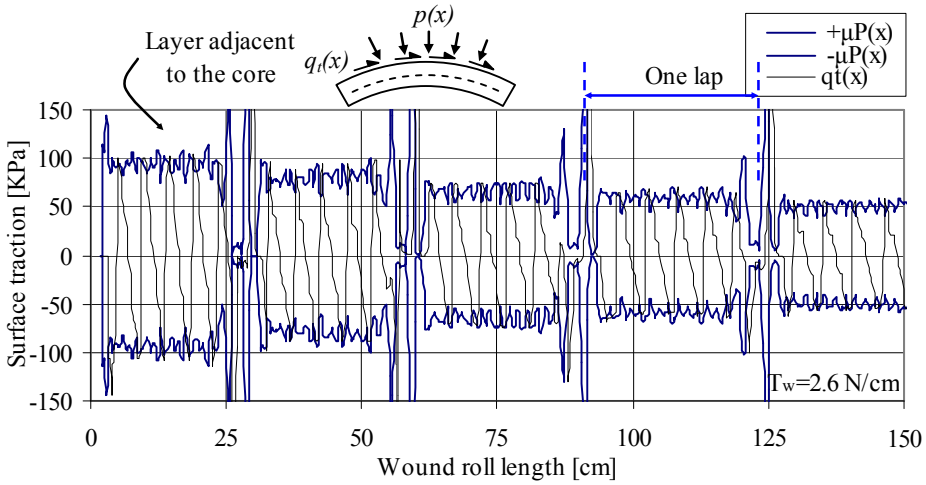

Figure 15 – Behavior of the top surface tractions in the layers near the core

The behavior of the surface traction indicates that most of the wound roll surface is under stick except at some discrete points where it slips. Between the slip points, the traction behaves linearly and the wound roll is in a condition of stick. It should be noted that the tractions in the top and bottom surface act opposite to each other and almost cancel each other except near the core and hence do not contribute to the in wound stresses. Due to the radial discontinuity near the core, the surface tractions do not completely cancel each other adding to the bending stresses created by the discontinuity.

CONCLUSIONS AND RECOMMENDATIONS

An explicit FE method has been used to model the wound roll structure of center wound rolls with and with out an undriven nip roller. The results of the FE model agree well with the results calculated using Hakiel's model in the part of the wound roll that is away from the core. Near the core, the FE model shows the increase in stresses due to the stress discontinuity caused by the spiral nature of the wound roll that has not previously been accounted for in wound roll models. The FE model results show that the NIT is proportional to the kinetic coefficient of friction between the web layers and is independent of the web tension. This is consistent with the observations of Good et al.

One of the advantages of using this type of modeling is the ability to analyze the forces and surface tractions that may cause slippage within the wound roll. For the cases discussed here, the surface tractions indicated that the layers within the wound roll were almost under complete stick. However, different frictional conditions may cause slippage within the wound roll. One of the limitations of this type of modeling is the computational time. Because the stable time increment in an explicit analysis is dependent on modulus, mass density, elemental dimensions and contact conditions, the total computational time is very high.

REFERENCES

1. Good, J. K., "The Abilities and Inabilities of Wound Roll Models to Predict Winding Defects", Proceedings of the Eight International Conference on Web Handling, Web Handling Research Center, Stillwater, Oklahoma, 2005.
2. Roisum, D. R., Mechanics of Winding, TAPPI Press, 1999.
3. Hoffecker, P. and J. K. Good, "Tension Allocation in Three Dimensional Axisymmetric Wound Roll Model", Proceedings of the Eighth International Conference on Web Handling, Web Handling Research Center, Oklahoma State University, Stillwater, Oklahoma, 2005.
4. Lee, Y. M. and J. A. Wickert, "Stress Field in Finite Width Axisymmetric Wound Rolls", ASME Journal of Applied Mechanics, Vol. 69 (2), 2002, pp. 130-138.
5. Smolinski, P., et al., "Modeling the collapse of coiled material", Finite Elements in Analysis and Design, Vol. 38 (6), 2002, pp. 521-535.
6. Li, S. and J. Cao, "A Hybrid Approach for Quantifying the Winding Process and Material Effects on Sheet Coil Deformation", Journal of Engineering Materials and Technology, Transactions of the ASME, Vol. 126 (3), 2004, pp. 303-313.
7. Arola, K. and von Hertzen, R., "Development of Sheet Tension under a Rolling Nip on a Paper Stack," International Journal of Mechanical Sciences, Vol. 47, 2005, pp. 110-133.
8. Arola, K. and von Hertzen, R., "An Elastoplastic Continuum Model for a Wound Roll with Interlayer Slippage," Finite Elements In Analysis and Design, Vol. 42, 2006, pp. 503-517.

9. Flanagan, D.P. and T. Belytschko, "A Uniform Strain Hexahedron and Quadrilateral with Orthogonal Hourglass Control", International Journal for Numerical Methods in Engineering, Vol. 17 (5), 1981, pp. 679-706.
10. ABAQUS Inc., ABAQUS Analysis User's Manual, 2005.
11. ABAQUS Inc., ABAQUS Theory Manual, 2005.
12. Belytschko, T., Liu, W. K., and Moran, B., Nonlinear Finite Elements for Continua and Structures, John Wiley & Sons, Ltd., 2000.
13. Belytschko, T., Chung, W. J., and Cho, J. W., "On the Dynamic Effects of Explicit FEM in Sheet Metal Forming Analysis," Engineering Computations, Vol. 15 (6), 1998, pp. 750-776.
14. Timeshenko, S.P. and Goodier, J. N., Theory of Elasticity, 3rd ed., McGraw Hill, 1970.
15. Hakiel, Z., "Nonlinear Model for Wound Roll Stresses," Tappi Journal, Vol. 70 (5), 1987, pp. 113-117.
16. Shigley, J.E. and Mischke, C. R., Mechanical Engineering Design, 4th ed., McGraw Hill, 1983.
17. Good, J. K. and Fikes, M. W. R., "Predicting the Internal Stresses in Center-Wound Rolls with an Undriven Nip Roller", TAPPI, Vol. 74 (6), 1991, pp. 101-109.
18. Good, J. K., Hartwig, J., and Markum, R., "A Comparison of Center and Surface Winding Using the Wound-In-Tension Method," Proceedings of the Fifth International Conference on Web Handling, Web Handling Research Center, Stillwater, Oklahoma, 1999, pp. 87-104.

Modeling Wound Rolls Using Explicit FE Methods	**B. K. Kandadai & J. K. Good**, Oklahoma State University, USA

Name & Affiliation	**Question**
Ron Swanson, 3M Corp.	I have a couple questions on the material properties. You employ a Young's modulus of 69 MPa that's almost two orders of magnitude lower than the modulus of polyester. Would the model run just as well for webs with larger Young's modulus? Was that value lower just to help calculations, or would it work just as well?
Name & Affiliation	**Answer**
B.K. Kandadai, Oklahoma State University	Correct. The value is about 10,000 psi. The reason I chose that value is that I was using an explicit code. The solution time is proportional to the modulus. So if you were to increase the modulus to simulate polyester with a modulus of 600,000 psi, your computational time would increase 60 times.
Name & Affiliation	**Question**
Ron Swanson, 3M Corp.	What value did you use for the radial modulus?
Name & Affiliation	**Answer**
B.K. Kandadai, Oklahoma State University	In this case I chose isotropic web properties, so the modulus was 10,000 psi in the radial direction as well. I could have chosen orthotropic properties. To accommodate the state dependency of the radial modulus on pressure or strain you can write a subroutine to update the properties after each solution step when the state variables are updated.
Name & Affiliation	**Question**
Bob Lucas, Winder Science	Was some of the noise that you had down in the earlier layers, be a function of the spring mass system of your nip roll bouncing and causing variations in wound-in-tension?
Name & Affiliation	**Answer**
B.K. Kandadai, Oklahoma State University	That is a very good question. I looked at that, but it is not. If you were to plot the surface traction as a function of time, as a function of the layers building, what you will see is that the surface tractions don't change, the first layer you wind, you've got significant stress concentration, significant out-of-roundness, so you can expect a lot of spring effects. As a function of time and the more layers that are wound on, you see the same surface traction behavior. So it eliminates the spring noise. Hence, it is the actual surface traction effect.
Name & Affiliation	**Question**
Jerry Brown, Essex Systems	What was the solution time for the example that you showed us?
Name & Affiliation	**Answer**
B.K. Kandadai, Oklahoma State University	2 ½ days. 5 years ago we couldn't simulate this on a PC. So 2 ½ days is tolerable.

Name & Affiliation	Question
Unknown	How many processors were used? Can these problems run using parallel processing?
Name & Affiliation	**Answer**
B.K. Kandadai, Oklahoma State University	These results were obtained using a single processor. We could have used multiple processors but the benefit in reduced solution time can be questionable. Some of the elements are not, for example, four node quadrilaterals with reduced integration which are not really suited for cluster computing, but in general it can be done.